Upstream Transmission in a Reflective FDMA-PON: results from the EU project FABULOUS

Upstream Transmission in a Reflective FDMA-PON: results from the EU project FABULOUS

J. Chang, R. Gaudino, V. Ferrero
Dipartimento Di Elettronica e Telecomunicazioni
Politecnico Di Torino,
Corso Duca degli Abruzzi, 24
10129 Turin, Italy

S. Straullu, P. Savio, A. Nespola, S. Abrate
Photonlab
Istituto Superiore Mario Boella,
Via Boggio 61
10138 Turin, Italy.

B. Charbonnier.
France Télécom Orange Labs,
2 av. Pierre Marzin,
22307 LANNION Cédex, France

***Abstract*— In this paper, we present a new FDMA-PON (Frequency Division Multiple Access – Passive Optical Network) architecture proposed by the FP7 EU STREP project titled "FABULOUS". The paper is focused on the upstream transmission, based on an innovative reflective optical network unit (R-ONU). A detailed theoretical analysis is first presented and used to optimize the system parameters, then we show the experimental results, demonstrating a 16 Gbps upstream bit rate per wavelength.**

Keywords—Optical communications, passive optical networks (PON), FDMA, Faraday Rotation, multiplexing techniques.

I. INTRODUCTION

The European project "FABULOUS" (Frequency Division Multiple Access By Using Low-cost Optical network Units in Silicon photonics) proposes a new architecture for next generation passive optical networks (PON) as described in details in [1] and [2]. The main characteristic in our architecture is the use of Frequency Division Multiple Access (FDMA), rather than the more traditional Time Division Multiple Access (TDMA) that is today applied in all ITU-T and IEEE PON standards, and the use of single-polarization coherent receivers for the upstream transmission, thanks to the polarization independent reflective modulation [6]. The several FDMA-PON architectures proposed in the literature, are usually characterized by a very high complexity in terms of both optoelectronic components requirements and digital signal processing (DSP). Furthermore, the recent standardized 10 Gbps TWDM-PON architecture targets 4 WDM wavelengths, each one with 2.5 Gbps upstream capacity. In our new architecture, we increase the capacity to 16 Gbps per wavelength, but maintaining a low complexity. For space limitations, this paper will focus only on the single wavelength upstream transmission, even though the project [2] targets also downstream transmission and WDM implementation.

The signal evolution in the FABULOUS upstream transmission is shown in Fig. 1; an un-modulated optical signal is generated in the central office (CO) by a continuous wave (CW) laser in the optical line terminal (OLT) and sent towards the optical distribution network (ODN). The signal reaches the optical network unit (ONU) and it is modulated by a reflective Mach-Zehnder modulator (R-MZM), which also performs a Faraday rotation. The electrical RF signal applied to the R-MZM carries *M-QAM* modulation and each RF *M-QAM* signal generated at each ONU has a bandwidth and a central frequency allocation to be spectrally separated with respect to the ones generated by the others ONUs sharing the same wavelength, as required by FDMA. Once the ONUs signals are modulated and recombined, they are sent back to the OLT, which is equipped with an optical coherent receiver followed by proper digital signal processing algorithms. Thanks to the Faraday effect performed at every ONU, all the upstream received signals have the same fixed polarization, orthogonal to the transmitted one, so that a simplified single-polarization optical receiver can be used without any polarization control.

The paper is organized as follows. Section II and III report a theoretical analysis of the upstream transmission. In Section IV we show some recent experimental results that confirms the theoretical analysis and shows an upstream bit rate of the order of 16 Gbps per wavelength.

I. THE UPSTREAM TRANSMISSION AND PERFORMANCE

A. The Reflective Mach-Zehnder Modulator

The R-MZM, shown in Fig. 2, is basically composed by a PBS (which splits the optical field into two orthogonal components) and a MZM (characterized by two independent electrodes) placed creating a ring configuration. Therefore, each component goes through opposite directions and is modulated by independent arms inside the modulator, as originally outlined in [4]. Interestingly, this allows a completely polarization independent reflective modulator that anyways need only single polarization waveguides internally, and thus, as outlined in [5], it is suitable for Silicon Photonic integration, which is one of the key targets of the FABULOUS

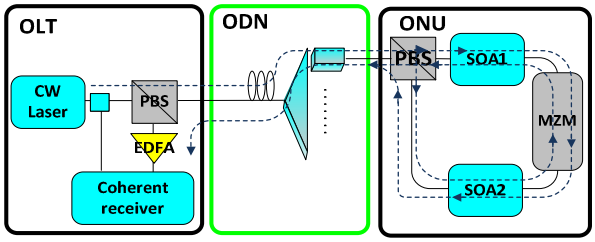

Fig. 1. Upstream signal evolution in the FABULOUS architecture.

project. The expressions related to the R-MZM input and output optical fields are shown in (1) and (2), where we assume that the input un-modulated optical field has a generic polarization and phase, described by the two random angles α and β, respectively. On the other hand, the output signal contains the modulating RF signal $V(t)$, normalized with respect to the modulator V_π, and the angle ϕ, which is the phase difference between the two MZM arms in absence of modulation.

$$\mathrm{E_{in}} = \sqrt{P_{in}} \cdot \begin{bmatrix} \cos(\alpha) \cdot e^{j\beta} \\ \sin(\alpha) \cdot e^{-j\beta} \end{bmatrix} \tag{1}$$

$$\mathrm{E_{out}} = \frac{\sqrt{P_{in}}}{2} \begin{bmatrix} Sin\alpha \cdot e^{-j\beta} \cdot (1 + e^{-j\cdot\pi\cdot V(t)} \cdot e^{-j\phi}) \\ Cos\alpha \cdot e^{j\beta} \cdot (e^{-j\cdot\pi\cdot V(t)} + e^{-j\phi}) \end{bmatrix} \tag{2}$$

By setting $\phi=\pi$ (the MZM biased at the minimum of its electro-optical characteristics), we perform the optical carrier suppression [4]. It can be easily shown that a polarization Faraday rotation is also generated and the expression from (2) is reduced to (3), where $\hat{E}_{in\perp}$ is the polarization orthogonal to the input field.

The expression (3) represents the FABULOUS R-MZM "ideal" modulation characteristic, where the output field moves on a circle in the complex plane.

$$E_{out} = \frac{\sqrt{P_{in}}}{2} \cdot \left(1 - e^{-j\cdot\pi\cdot V(t)}\right) \cdot \hat{E}_{in\perp} \tag{3}$$

B. Nonlinearity of the MZM

Using (3), we will study the intrinsic nonlinear effects of this kind of modulator. We use the modulation index (m_{index}) as a reference parameter and it is defined as the ratio between the maximum driving RF signal level and the MZM half wave voltage (specifying the voltage swing in the modulator).

$$m_{index} = V_{\max} / V_\pi \tag{4}$$

As a first approach to assess the device nonlinearity , we consider a sinusoidal input signal with frequency fm so that the driving signal is represented as (5). Substituting it on (3), and using the properties of the Fourier Transform and the Bessel functions, the output field can be written as (6).

$$V(t) = m_{index} \cdot \sin(2\pi f_m t) \tag{5}$$

$$E_{out} = \frac{E_{in}}{2} \cdot [1 - \sum_{n=-\infty}^{\infty} J_n(\pi \cdot m) \cdot e^{j\cdot 2\cdot n\cdot\pi\cdot f_m\cdot t}] \tag{6}$$

From this equation, we observe the presence of several spectral components: the DC component (n=0), the useful signal (n=1) and its spurious harmonics (n>1), that in the case of using modulated signals, would interfere with channels transmitted at different frequencies inside the FDM scheme. For a more realistic approach, using a modulated signal (i.e. *M-QAM*) will be somehow similar to a sinusoidal modulation but with variable phase and amplitude. However, there is no easy close form to express the nonlinearity for the modulated case, so we evaluate it through numerical simulations as shown in section III. The modulation formats considered are: *QPSK*, *16-QAM* and *64-QAM*.

C. Performance assessment and required signal to noise ratio

In order to assess the system performance for the three different modulation formats, the error vector magnitude (EVM) is taken as a reference parameter, since it is easily estimated from the scattering diagrams and it is directly related to the performance in terms of bit error rate (BER) [3]. In order to guarantee BER = 10^{-3}, the required EVM values for *QPSK*, *16-QAM* and *64-QAM* are 30%, 10% and 5%, respectively. Correspondingly, due to the relation between the electrical signal to noise ratio (E_b/N_0, bit energy over the noise level) and the system performance, to target BER of 10^{-3} the required E_b/N_0 would be: 6.8dB (*QPSK*), 10.5dB (*16-QAM*) and 14.7dB (*64-QAM*).

II. Simulations

A. Computation using a sinusoidal input signal

In order to perform an analysis regarding the R-MZM nonlinearity using a sinusoidal input signal, we perform the calculation using (6), obtaining the different components relative power levels, with respect to the output useful signal, and the "modulation attenuation", defined as the ratio between the output useful signal and the input optical power at the PBS (excluding the R-MZM intrinsic passive loss). The results are shown in Fig. 3. We observe that by increasing m_{index}, the nonlinearity increases since the spurious signals grow faster than the useful one. The DC component is the strongest but would not create crosstalk on other modulated signals (the lower part of the electrical spectrum below approximately 1GHz is not used in our architecture), while the most relevant

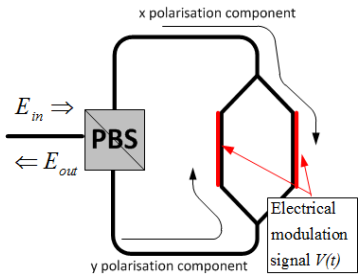

Fig. 2. Reflective Mach-Zehnder Modulator structure to be integrated in Silicon Photonic technology.

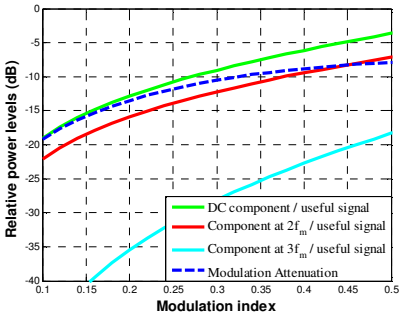

Fig. 3. Relative Power levels related to the useful signal using a sinusoidal input.

spurious signal is at the second harmonic; the third harmonic, that is much lower, can be neglected. On the other hand, by increasing m_{index}, the modulation attenuation reduces instead. This means that an optimum value can be found by establishing a balance between these two different trends.

B. *Simulation using different modulation formats*

In this part, we introduce time-domain simulations where instead of using a sinusoidal signal, we simulate several modulation formats that may be used in FABULOUS: *QPSK*, *16-QAM* and *64-QAM*. For these numerical simulations, we set the data rate at 1Gbps, the modulating frequency f_m at 2GHz, a pulse shaping with an square-root-raised-cosine (SRRC) filter with 0.1 of roll-off (r), and an ideal modulator (with perfect symmetry and biasing point). Following the same analysis done in the previous subsection, the nonlinear behavior is similar to the sinusoidal case but each component here is modulated. We evaluate the relative power levels for the three modulation formats, focusing on the second harmonic relative power (which may cause potential crosstalk on another channel in the environment with several ONUs) and the modulation attenuation. The simulation outcomes are shown in Fig. 4 and Fig. 5. Comparing the results with those obtained under sinusoidal modulation (previous subsection), we can see that the trends are the same, and in particular as we increase m_{index} the relative power increases and for the same value of m_{index} this power ratio is anyway smaller for the modulated case (around 7 dB better). On the other hand, in the *M-QAM* modulated case, the modulation attenuation is higher due to the fact that the sinusoidal signal is always at its peak power, so its level is higher if compared to the modulated *M-QAM* signal's envelope.

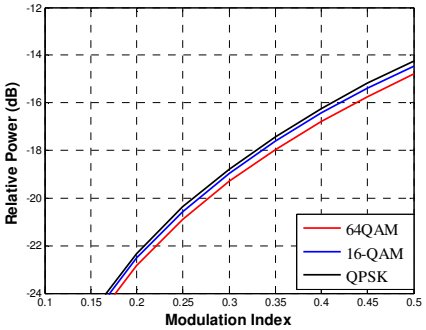

Fig. 4. Relative Power level of the 2*fm* component over the useful signal for the QPSK, 16-QAM and 64 QAM modulation formats.

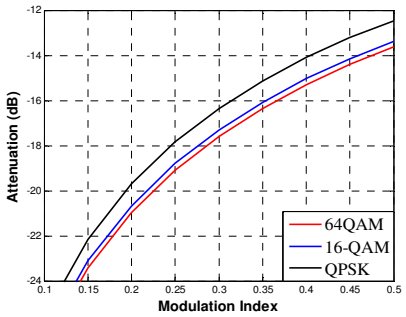

Fig. 5. Modulation Attenuation for the QPSK, 16-QAM and 64 QAM modulation formats.

C. *Simulation with an interferent channel*

In the previous two subsections we have considered a single channel upstream transmission. In this part, we study the simultaneous transmission by several ONUs sharing the same wavelength, the case where nonlinearity becomes fundamental. We point out that the spurious due to the second harmonic of the adjacent channels do not overlap spectrally the channel under test (the nonlinear effects does not increase when increasing the number of users in the system), so it is enough to analyze the system with two channels: the channel under observation and the other generating the interference.

The worst-case situation is when a channel transmitting at *fm* generates the spurious component at 2*fm* that coincides with the central frequency of another channel. This simulation is done under the following assumptions: ideal R-MZM, two independent users transmitting with central frequencies at 1GHz and 2GHz (the one under evaluation), data rate at 1Gbps, SRRC pulse shaping with r = 0.1 and the presence of white Gaussian noise (WGN) at the receiver (set specifically for each modulation format in order to limit the system at the target BER of 10^{-3}, see section II.C).

The results are shown in Fig. 6 and we can see that at the limits of each modulation format (5%, 10% and 30%, respectively to guarantee BER=10^{-3}), the optimal m_{index} is when the trade-off between the crosstalk interference and the WGN is satisfied: for small values of m_{index} the system is limited by the noise and for higher values by the modulator nonlinearity. For more complex modulation formats, as *M-QAM*, the nonlinearity impact is higher, thus *QPSK* has an optimal m_{index} value of 0.5, which is higher and more robust in

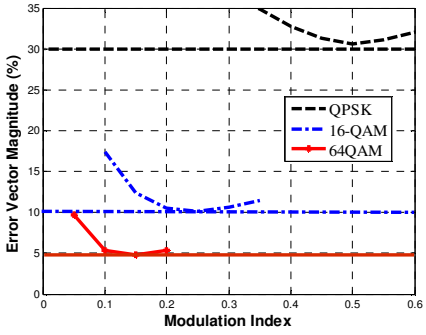

Fig. 6. Optimum values of modulation index for *QPSK*, *16-QAM* and *64QAM*. The limits for BER=10-3 are reported with horizontal lines.

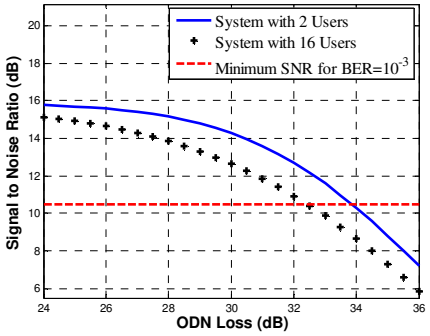

Fig. 7. Received SNR vs. ODN loss for *16-QAM*. The required SNR level for BER=10-3 is reported as a red dashed line.

terms of interference (due to spurious second harmonics) and required signal to noise ratio (lower modulation attenuation) with respect to the other formats. On the other hand for *16-QAM* and *64-QAM* require the reduction of m_{index} to 0.25 and 0.15 respectively, which means an increase of modulation attenuation. However, since it is required high data rates (high spectral efficiency) and an achievable signal to noise ratio (thus lower modulation attenuation), we focus our analysis on the *16-QAM* format.

D. Power Budget Analysis

We analytically estimated the power budget for a system using *16-QAM* transmitting at 1Gbps per user, analyzing the signal to noise ratio of the complete system from the un-modulated signal generated by the OLT, to the received back signal modulated by the ONU. This activity was very important to understand the ultimate physical layer system limitations, and to drive the experimental setup shown later.

The received available SNR is computed by evaluating the signal and noise evolutions inside the system's path. For the signal, we consider a first order analysis that takes into account only optoelectronic devices losses while, for the noise calculation we considered the ASE noise generated by the optical amplifiers in the system, i.e. the semiconductor optical amplifiers (SOA) at the ONU side and the EDFA at the OLT side. Moreover, we consider as an additional noise source the interference from other channels, caused by the modulator nonlinearity (the second harmonic generations).

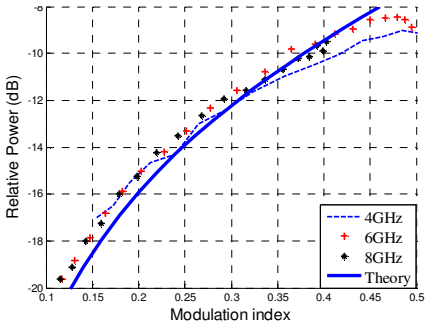

Fig. 8. Experimental characterization of the relative power level of the 2*fm* component over the useful signal

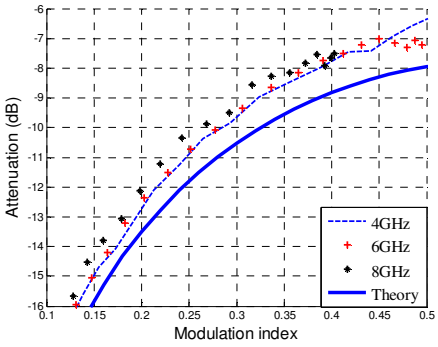

Fig. 9. Experimental characterization of the modulation attenuation.

It is important to mention that the overall ASE noise is the most relevant noise contribution for our system, indeed it is due to the total contribution of all the system's ONUs sharing the same wavelength. The simulation schematic is shown in Fig. 1. The launched CW signal power is 5dBm @1550nm (at the OLT output), the loss due to each PBS is 1dB, the internal loss of the MZM is 4dB, with a modulation attenuation of 21dB and an interference due to second harmonic generation of 22dB below useful signal (working at m_{index} = 0.2, see previous figures), the ONU SOA gain is 18dB with 9dB of noise figure, and the EDFA gain is 16dB with 5dB of noise figure. By varying the ODN loss and setting the number of users to 2 and 16, the simulations are performed and the results are shown in Fig. 7 in terms of received signal to noise ratio vs. ODN loss. We can see that the system with these characteristics could reach significant levels of ODN loss as required by the ITU-T standard for XGPON, and in particular the "ODN loss classes" "Nominal 1 (N1)" and "Nominal 2 (N2)", which specify a maximum ODN loss of 29dB and 31dB, respectively.

III. EXPERIMENTAL RESULTS

In this section, we support the theoretical analysis and simulations presented in previous sections with experimental results. As planned in the current first phase of the EU project FABULOUS, these experiments use commercial discrete optoelectronic components. The second phase of the project will introduce in 2015 an ONU integrated version realized in a Silicon Photonics platform.

A. Experimental results using sinusoidal input signals

In order to verify the simulations presented on III.A when a sinusoidal driving signal is used, we carry out the related experimental measurements. By using an optical spectrum analyzer, we measured the modulation attenuation and the relative power level with respect to the second harmonic, showing the results in Fig. 8 and 9. The modulator nonlinearity was a little different with respect to the theory. We can observe the agreement between the computation and the measurements of the relative power regarding the second harmonic. On the other hand, the modulation attenuation was slightly lower than the computed one (the power transferred to the spurious harmonics was lower).

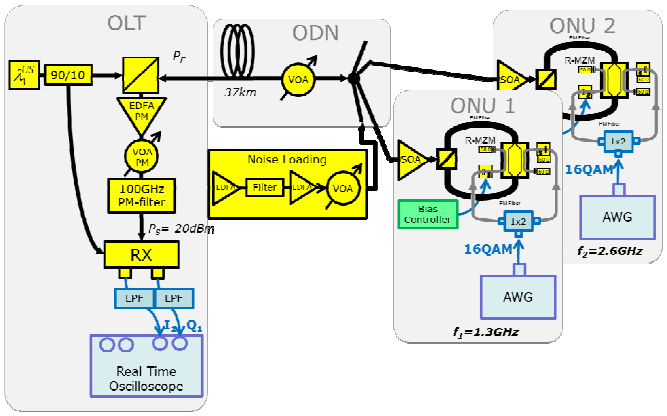

Fig. 10. Experimental setup with two ONUs and noise loading.

B. *Experimental results using 16-QAM input signals*

The second set of measurements refer to a realistic experimental system with 2 ONUs shown in Fig. 10 that uses *16-QAM* modulation format at 1 Gbps net data rate and noise loading in order to emulate the other additional users' ASE contribution. The OLT launch power is 5dBm; the two ONUs are transmitting in a worst-case frequency allocation (at 1.3GHz and 2.6GHz and the measurements are taken at the higher harmonic) with a data rate of 1Gbps and SRRC pulse shaping with r = 0.1. The performance in terms of m_{index} and ODN loss (for two ONUs case) is presented in Fig. 11. We see that the optimum m_{index} coincides with the same value estimated in the previous sections (around 0.2). On the other hand, the maximum reachable ODN loss of 26.8dB is lower than the expected value from the simulations; this is due to the nonlinearity introduced by the SOA used for the amplification in both co-propagating and counter-propagating directions inside every ONU, which generates additional spurious components that were not taken into account in the simulations. Setting the optimum modulation index, we evaluate the performance in terms of ODN loss vs. the number of users and the experimental results are presented in Fig. 12.

We point out that in order to guarantee BER= 10^{-3} the FABULOUS architecture is able to supply 16 users corresponding to 16Gbps capacity per wavelength with 24dB of ODN loss. However, the performance can be improved by introducing a better frequency allocation, so second harmonics do not fall exactly into the center frequency of other channels.

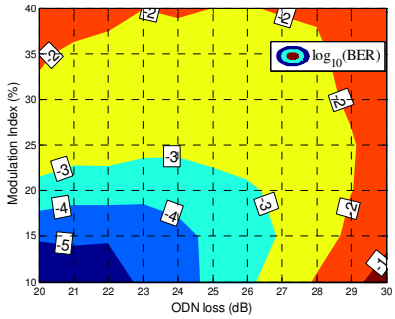

Fig. 11. Performance of the system for 2 users in the worst-case frequency allocation (1.3 and 2.6 GHz).

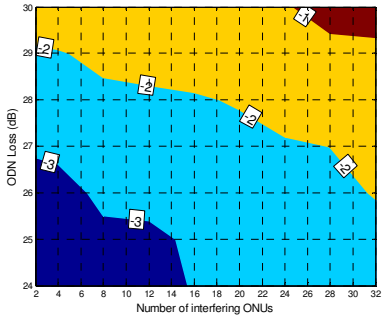

Fig. 12. Performance of the system vs. Number of users in the worst-case frequency allocation (1.3 and 2.6 GHz).

As an example, by setting the modulating frequencies at 1.4GHz and 2.6GHz the performance can increase without adding complexity.

IV. CONCLUSIONS

We have demonstrated the upstream FABULOUS architecture feasibility with 16 Gbps capacity per wavelength, higher with respect to the standard TWDM-PON. In details, we presented the analysis of the R-MZM and showed its impact on the performance in terms of modulation attenuation and interference to other channels. Similarly, we obtained the optimum m_{index} for each modulation format by evaluating the trade-off between the modulator nonlinearity, modulator attenuation and the equivalent ASE noise of the full system. From this, it is determined that the *16-QAM* modulation format is suitable for the FABULOUS scenario in order to guarantee the required signal to noise ratio and to limit the crosstalk between channels. The optimum m_{index} in this case was demonstrated to be 0.2.

ACKNOWLEDGMENT

This work was realized in the framework of the FP7 FABULOUS EU-STREP Project, contract n. 318704.

REFERENCES

[1] www.fabulous-project.eu

[2] S. Abrate, R. Gaudino, B. Charbonnier, "FDMA-PON architecture according to the FABULOUS European Project", Proc. SPIE 8645, Broadband Access Communication Technologies VII, 864504, January 4, 2013.

[3] R. Schmogrow, et al., "Error Vector Magnitude as a Performance Measure for Advanced Modulation Formats", *IEEE PHOTONICS TECHNOLOGY LETTERS* VOL. 24, NO. 1, January 2012

[4] B. Charbonnier, A. Lebreton, S. Straullu, V. Ferrero, A. Sanna, R. Gaudino, "Self-Coherent single wavelength SC-FDMA PON uplink for NG-PON2", Optical Fiber Communication Conference, OFC 2012, Los Angeles, 2012.

[5] B. Charbonnier, S. Menezo, P. O'Brien, A. Lebreton, J. M Fedeli, B. Ben Bakir, "Silicon photonics for next generation FDM/FDMA PON", *Optical Communications and Networking, IEEE/OSA Journal of* , vol.4, no.9, pp.A29,A37, Sept. 2012

[6] B. Charbonnier, N. Brochier, P. Chanclou, "Reflective polarisation Mach-Zenhder modulator for FDMA/OFDMA PON", Electronics Letters, vol. 46, no. 25, December 2010.